Published OnlineFirst March 24, 2015; DOI: 10.1158/1940-6207.CAPR-14-0362

Research Article

Cancer Prevention Research

Nrf2 Activation Protects against Solar-Simulated Ultraviolet Radiation in Mice and Humans

Elena V. Knatko[1], Sally H. Ibbotson[2], Ying Zhang[1], Maureen Higgins[1], Jed W. Fahey[3,4], Paul Talalay[3], Robert S. Dawe[2], James Ferguson[2], Jeffrey T.-J. Huang[1], Rosemary Clarke[5], Suqing Zheng[6], Akira Saito[6], Sukirti Kalra[1], Andrea L. Benedict[3], Tadashi Honda[6,7], Charlotte M. Proby[1,2], and Albena T. Dinkova-Kostova[1,3]

Abstract

The transcription factor Nrf2 determines the ability to adapt and survive under conditions of electrophilic, oxidative, and inflammatory stress by regulating the expression of elaborate networks comprising nearly 500 genes encoding proteins with versatile cytoprotective functions. In mice, disruption of Nrf2 increases susceptibility to carcinogens and accelerates disease pathogenesis. Paradoxically, Nrf2 is upregulated in established human tumors, but whether this upregulation drives carcinogenesis is not known. Here we show that the incidence, multiplicity, and burden of solar-simulated UV radiation–mediated cutaneous tumors that form in SKH-1 hairless mice in which Nrf2 is genetically constitutively activated are lower than those that arise in their wild-type counterparts. Pharmacologic Nrf2 activation by topical biweekly applications of small (40 nmol) quantities of the potent bis(cyano enone) inducer TBE-31 has a similar protective effect against solar-simulated UV radiation in animals receiving long-term treatment with the immunosuppressive agent azathioprine. Genetic or pharmacologic Nrf2 activation lowers the expression of the pro-inflammatory factors IL6 and IL1β, and COX2 after acute exposure of mice to UV radiation. In healthy human subjects, topical applications of extracts delivering the Nrf2 activator sulforaphane reduced the degree of solar-simulated UV radiation–induced skin erythema, a quantifiable surrogate endpoint for cutaneous damage and skin cancer risk. Collectively, these data show that Nrf2 is not a driver for tumorigenesis even upon exposure to a very potent and complete carcinogen and strongly suggest that the frequent activation of Nrf2 in established human tumors is a marker of metabolic adaptation. *Cancer Prev Res; 8(6); 475–86.* ©*2015 AACR.*

Introduction

The cap'n'collar (CNC) basic-region leucine zipper (bZIP) transcription factor NF-E2 p45-related factor 2 (Nrf2, also called Nfe2l2) orchestrates a transcriptional program comprising nearly 500 genes encoding cytoprotective proteins, which allow adaptation and survival under conditions of electrophilic and oxidative stress (1–3). The diverse functions of the transcriptional targets of Nrf2 include antioxidant and drug-metabolizing enzymes, as well as proteins that participate in glucose, lipid, and nucleotide metabolism, placing this transcription factor at the interface between cellular redox and intermediary metabolism (4). Under homeostatic conditions, Nrf2 is mainly regulated by Kelch-like ECH-associated protein 1 (Keap1), a Cullin (Cul)-3/Rbx1 ubiquitin ligase substrate adaptor protein that mediates continuous ubiquitination and proteasomal degradation of the transcription factor (5–7). In addition to being a repressor for Nrf2, Keap1 is also the cellular sensor for a wide array of sulfhydryl-reactive small molecules (termed inducers) that chemically modify the sensor cysteines of Keap1, leading to loss of repressor function, Nrf2 stabilization, and upregulation of downstream target gene expression (8, 9). A large body of experimental evidence has demonstrated that the absence of Nrf2 increases the sensitivity to numerous carcinogens and accelerates disease progression. Conversely, Nrf2 activation by pharmacologic agents protects against cancer in various animal models. Paradoxically however, Nrf2 is frequently activated in human tumors and contributes to resistance to chemotherapy and radiation therapy (10, 11).

Non-melanoma skin cancers are the most common human malignancies, with more than 2 million new cases diagnosed globally each year (12). Furthermore, cutaneous squamous cell carcinomas (cSCC) are among the most highly mutated human cancers, carrying one mutation per ∼30,000 bp of coding sequence (13). The risk for cSCC is particularly high and its

[1]Jacqui Wood Cancer Centre, Division of Cancer Research, Medical Research Institute, University of Dundee, Dundee, Scotland, United Kingdom. [2]Photobiology Unit, Ninewells Hospital and Medical School, University of Dundee, Dundee, Scotland, United Kingdom. [3]Lewis B. and Dorothy Cullman Chemoprotection Center, Department of Pharmacology and Molecular Sciences, Johns Hopkins University School of Medicine, Baltimore, Maryland. [4]Center for Human Nutrition, Department of International Health, Johns Hopkins University Bloomberg School of Public Health, Baltimore, Maryland. [5]Division of Cell Signaling and Immunology, College of Life Sciences, University of Dundee, Dundee, Scotland, United Kingdom. [6]Institute of Chemical Biology and Drug Discovery, Stony Brook University, Stony Brook, New York. [7]Department of Chemistry, Stony Brook University, Stony Brook, New York.

Note: Supplementary data for this article are available at Cancer Prevention Research Online (http://cancerprevres.aacrjournals.org/).

Corresponding Author: Albena T. Dinkova-Kostova, Division of Cancer Research, Medical Research Institute, James Arrott Drive, Ninewells Hospital and Medical School, Dundee DD1 9SY, United Kingdom. Phone: 44-1382-383386; Fax: 44-1382-669993; E-mail: a.dinkovakostova@dundee.ac.uk

doi: 10.1158/1940-6207.CAPR-14-0362

Published OnlineFirst March 24, 2015; DOI: 10.1158/1940-6207.CAPR-14-0362

management is especially problematic in specific high-risk groups, such as solid organ transplant recipients receiving life-long immunosuppressive therapies, for whom skin cancer is a major cause of morbidity and mortality (14). Solar ultraviolet (UV) radiation, the most abundant carcinogen in our environment, is the main factor in the etiology of cSCC, both in the general and the immunosuppressed populations, causing generation of reactive oxygen species (ROS), direct and indirect (oxidative) DNA damage, inflammation, and immunosuppression. Most of these damaging processes are counteracted by the endogenous cytoprotective mechanisms that are regulated by Nrf2. It has been previously shown that small-molecule activators of Nrf2 protect against UVA- or UVB radiation–induced damage in cells and *in vivo* (15). In female C57BL/6 and CD-1 mice, the Nrf2 activator sulforaphane protects against oncogenic H-Ras(Q61L)-driven papilloma formation in the 7,12-dimethylbenz[*a*]anthracene/12-*O*-tetradecanoylphorbol-13-acetate (DMBA/TPA) model (16, 17). Topical or dietary administration of sulforaphane-rich broccoli sprout extracts is also protective against UVB radiation–mediated skin carcinogenesis in female SKH-1 hairless mice (18, 19). However, it is unclear whether this protection extends to solar UV radiation, which comprises both UVA and UVB wavelengths and is much more relevant to human exposure to sunlight than either UVA or UVB individually. Furthermore, it is not known whether pharmacologic activation of Nrf2 protects against the development of cSCC caused by solar UV radiation under conditions of life-long immunosuppressive therapy. In addition, given that Nrf2 is often activated in established tumors, a critical question arises whether constitutive Nrf2 activation could be a driver for tumor development.

To address these questions, we generated SKH-1 hairless mice in which Nrf2 is either disrupted or constitutively activated. SKH-1 hairless mice are immunocompetent but have a defect in the hairless (*Hr*) gene encoding a transcriptional corepressor, the loss of which renders the animals hairless after completion of the first hair cycle (20). By use of these new mouse models, we found that genetic activation of Nrf2 protects against skin carcinogenesis evoked by solar-simulated UV radiation, indicating that constitutive Nrf2 activation does not drive cutaneous tumor development even upon exposure to a complete (both an initiator and a promoter) carcinogen. We further show that topical twice-weekly applications of small (nanomol) quantities of the potent pharmacologic Nrf2 activator TBE-31, a tricyclic bis(cyano enone) (21), greatly reduces the multiplicity and volume of tumors that form after chronic exposure to solar-simulated UV radiation in SKH-1 hairless mice receiving the immunosuppressive agent azathioprine. In addition, in healthy human subjects, topical application of extracts containing an Nrf2 activator, sulforaphane, reduced the degree of skin erythema following acute exposure to solar-simulated UV radiation.

Materials and Methods

Materials

All chemicals and reagents were obtained from common commercial suppliers and were of the highest purity available. (±)-TBE-31 was synthesized as described (21, 22). A stable isotope labeled (±)-[$^{13}C_2{}^{15}N_2$]-TBE-31 was synthesized in four steps from a previously reported intermediate (22), which is prepared in 11 steps from cyclohexanone, by introduction of two ^{13}C atoms with ethyl [^{13}C]formate and two ^{15}N atoms with hydroxy[^{15}N]amine (23).

Animals and treatments

All animal experiments were performed in accordance with the regulations described in the UK Animals (Scientific Procedures) Act 1986, and were in strict compliance with institutional guidelines. SKH-1 hairless mice were initially obtained from Charles River and then bred in our facility with free access to water and food (pelleted RM1 diet from SDS Ltd.), on a 12-hour light/dark cycle, 35% humidity. Nrf2-KO and Keap1-KD SKH-1 hairless mice were generated by back-crossing Nrf2-KO (24) and Keap1-KD (25) C57BL/6 mice onto the SKH-1 hairless genetic background over six generations. All experimental animals were age-matched and female.

For experiments with azathioprine, the animals were housed in individually ventilated cages. Azathioprine (Sigma-Aldrich Co) was freshly prepared in 0.05 N NaOH and diluted at a ratio of 1:500 (v/v) into the drinking water to a final concentration of 61.25 μg/mL, resulting in the animals receiving azathioprine at a dose of 1 mg/kg/d. The water bottles were changed 3 times per week and were kept wrapped in aluminum foil to protect azathioprine from light exposure. TBE-31 was applied topically in 200 μL of 80% acetone (v/v) over the entire back (dorsal skin) of the mouse. Control mice received 200 μL of 80% acetone (v/v). At the end of each experiment, the animals were euthanized, and blood was drawn by cardiac puncture and collected in Eppendorf tubes containing 5 μL of 500 mmol/L EDTA. Plasma was obtained by centrifugation at 25°C (300 × *g* for 20 minutes) and immediately frozen in liquid N_2. Skin, liver, and kidneys were harvested immediately after blood draw, frozen in liquid N_2, and stored at −80 °C until analysis. For TBE-31 pharmacokinetic experiments, harvested dorsal skin from the site of application was first rinsed in PBS, blotted on filter paper, and then frozen.

Exposure of mice to solar-simulated UV radiation

The UV lamps (UVA340, Q-Lab) used to irradiate the animals provide a near-perfect simulation of sunlight in the critical short wavelength region, from 365 nm to the solar cutoff of 295 nm, with a peak emission at 340 nm (Supplementary Fig. S1). The radiant dose was quantified, at the appropriate distance, with a UVB Daavlin Flex Control Integrating Dosimeter and further confirmed with an external radiometer (X-96 Irradiance Meter, Daavlin) before and after each irradiation session. An electrical fan was used to avoid excessive heating. For acute radiation experiments, the animals were exposed to UV radiation in groups and euthanized 24 or 72 hours after irradiation. Dorsal skin was harvested, immediately frozen in liquid N_2, and stored at −80 °C.

For skin carcinogenesis experiments, the animals were exposed twice a week for 15 weeks on Tuesdays and Fridays to solar-simulated UV radiation (comprised of 2 J/cm^2 UVA and 90 mJ/cm^2 UVB) in clear bedding-free cages. For the study comparing the three genotypes of mice, the animals were randomized in such a way that every cage contained representatives of each genotype. Treatment with TBE-31 (40 nmol per mouse, applied topically in 200 μL of 80% acetone v/v over the entire back of the animal, biweekly, on Mondays and Thursdays or 200 μL of 80% acetone vehicle control) and azathioprine (1 mg/kg, daily, *per os*) began 2 weeks before the first exposure to UV radiation and continued throughout the experiment. Tumors (defined as lesions >1 mm in diameter) and body weights were recorded

Published OnlineFirst March 24, 2015; DOI: 10.1158/1940-6207.CAPR-14-0362

weekly. Tumor volumes ($v = 4\pi r^3/3$) were determined by measuring the height, length, and width, and using the average of the three measurements as the diameter.

Biochemical analyses

Frozen tissue was pulverized into powder under liquid N_2. The powder was weighed and about 30 mg was resuspended in ice-cold buffer (100 mmol/L potassium phosphate, pH 7.4; 100 mmol/L KCl; 0.1 mmol/L EDTA), homogenized in an ice bath, and subjected to centrifugation at 4°C (15,000 × *g* for 10 minutes). The enzyme activities of NQO1 with menadione as a substrate (26) and of GST with CDNB as a substrate (27) were determined in supernatant fractions. Protein concentrations were measured by the bicinchoninic acid (BCA) assay (Thermo Scientific).

For Western blot analysis of the levels of Keap1, Nrf2, and GCLC, skin powder (~30 mg) was resuspended and homogenized in ice-cold radioimmunoprecipitation assay buffer (50 mmol/L Tris-HCl, pH 7.5; 150 mmol/L NaCl; 1% NP-40; 0.5% sodium deoxycholate; 0.1% SDS; 1 mmol/L EDTA, with added EDTA-free protease inhibitors cocktail; Roche). Proteins were separated by electrophoresis on a 10% SDS-PAGE and then electrophoretically transferred to immobilon-P membrane (Millipore). After blocking with 10% non-fat milk at 4°C for 2 hours, immunoblotting was performed using the following antibodies: rabbit polyclonal Nrf2 antibody at a dilution of 1:2,000, rabbit polyclonal Keap1 antibody at a dilution of 1:2,000, or sheep GCLC antibody at a dilution of 1:2,500 (all kind gifts from John D. Hayes, University of Dundee, Dundee, UK; ref. 28). Antibodies against GAPDH (Sigma-Aldrich Co.; 1:5,000 dilution) or β-actin (Sigma-Aldrich Co.; 1:10,000 dilution) were used as loading controls.

Quantitative real-time PCR

The primers and probes (TaqMan Gene Expression Assays) used to measure the mRNA levels for Keap1, Nrf1, Nrf3, NQO1, GSTP, GCLC, HMOX-1, IL6, IL1β, and COX2 were from Life Technologies. Total RNA was extracted from mouse skin using RNeasy Fibrous Tissue Kit (Qiagen Ltd.). Omniscript RT Kit (Qiagen Ltd.) was then used to reverse-transcribe 500 ng of total RNA into cDNA. Real-time PCR was carried out on Perkin Elmer/Applied Biosystems Prism Model 7700 Sequence Detector instrument. The TaqMan data for the mRNA species were normalized using β-actin (mouse ACTB, 4352933E) as an internal control.

Extract treatment and exposure of healthy human subjects to solar-simulated UV radiation

The human study was approved by the East of Scotland Research Ethics Service and the Institutional Review Board of Johns Hopkins University (Baltimore, MD). Informed consent was obtained from each participant after the nature and possible consequences of the study were fully explained. The extracts were prepared and analyzed as described in Supplementary Methods (26, 29) and dispensed in containers wrapped in aluminum foil that do not state their contents (marked "L" and "M"). Thus, subjects, assessors, and those applying the extracts did not know which was active and which was placebo. To determine which side (left or right) of the back is to receive active and which placebo, a random allocation sequence was produced using blocked computerized random allocation, with allocations for each subject concealed in an opaque envelope. On days 1 to 3, after gently cleaning the skin with isopropyl alcohol, the right or the left half of the mid-upper back skin of each volunteer received, as randomly allocated, active or placebo extracts (delivering 200 nmol/cm^2 of sulforaphane or glucoraphanin), respectively, 3 times, 24 hours apart. On day 4, the extract-treated areas were washed gently with saline followed by isopropyl alcohol to remove any residual surface extract. Then, small areas of the skin (approximately 1 cm^2) within the treated areas were exposed to a range of doses of UV and visible light from a monochromator 450W xenon arc source (at specific wavebands centered on 305, 335, 365, and 400 nm), and solar-simulated UV radiation from a 150W xenon arc filtered source, the emission spectrum of which approximates the mid-day summer solar spectrum. The intensity of erythemal responses at the active- and placebo-treated sites was determined 24 hours later—assessing threshold erythema response (minimal erythema dose, MED) and overall sum of intensity of erythema. MED was defined as the dose required to give minimal perceptible redness. It was planned to go onto a study to assess whether or not there might be changes in human tissue associated with photoprotection only if with at least one of the wavebands tested in the human study there was a photoprotection factor of ≥1.4 and/or a change of erythema of ≥ to 20% detected.

Statistical analysis

Values are means ± 1 SD or 1 SEM, as indicated in the figure legends. The differences between groups were determined by the Student *t* test or by ANOVA, as indicated in the figure legends. Analyses were performed using either Excel (Microsoft Corp.) or Stata 11.2 (Statacorp).

Results

Genetic upregulation of Nrf2 protects against inflammation caused by solar-simulated UV radiation

We generated SKH-1 hairless mice in which Nrf2 is either disrupted or constitutively activated by back-crossing Nrf2-knockout (Nrf2-KO; ref. 24) and Keap1-knockdown (Keap1-KD; ref. 25) C57BL/6 mice onto the SKH-1 hairless genetic background over six generations. Keap1-KD mice carry two floxed alleles of the *keap1* gene, which reduces its expression and consequently increases the levels of Nrf2, and thus represent a genetic model for constitutive Nrf2 activation (25). The mRNA and protein levels of Keap1 in samples isolated from skin of Nrf2-KO SKH-1 hairless mice are comparable with those of wild-type (WT) animals; however, the mRNA levels of Keap1 are 75% lower, and the protein levels are also reduced by about 60% in their Keap1-KD counterparts (Fig. 1A and B). As expected, Nrf2-KO SKH-1 hairless animals have no detectable Nrf2 levels in their skin, whereas skin isolated from Keap1-KD SKH-1 hairless mice has about 2-fold higher levels of the transcription factor compared with WT (Fig. 1C). The specific activity of the Nrf2-dependent enzyme NAD(P)H:quinone oxidoreductase 1 (NQO1) is about 30% lower ($P < 0.05$) in Nrf2-KO compared with WT skin, whereas it is 2.2-fold higher in Keap1-KD skin ($P < 0.001$; Fig. 1D). Similarly, compared with WT, the specific activity of cutaneous glutathione *S*-transferase (GST), another Nrf2 target enzyme, is reduced by about 40% in Nrf2-KO mice ($P < 0.05$) and upregulated by 1.3-fold in Keap1-KD animals ($P < 0.05$; Fig. 1D). The protein levels of the catalytic subunit of γ-glutamyl cysteine ligase (GCLC), an Nrf2-dependent enzyme which

Published OnlineFirst March 24, 2015; DOI: 10.1158/1940-6207.CAPR-14-0362

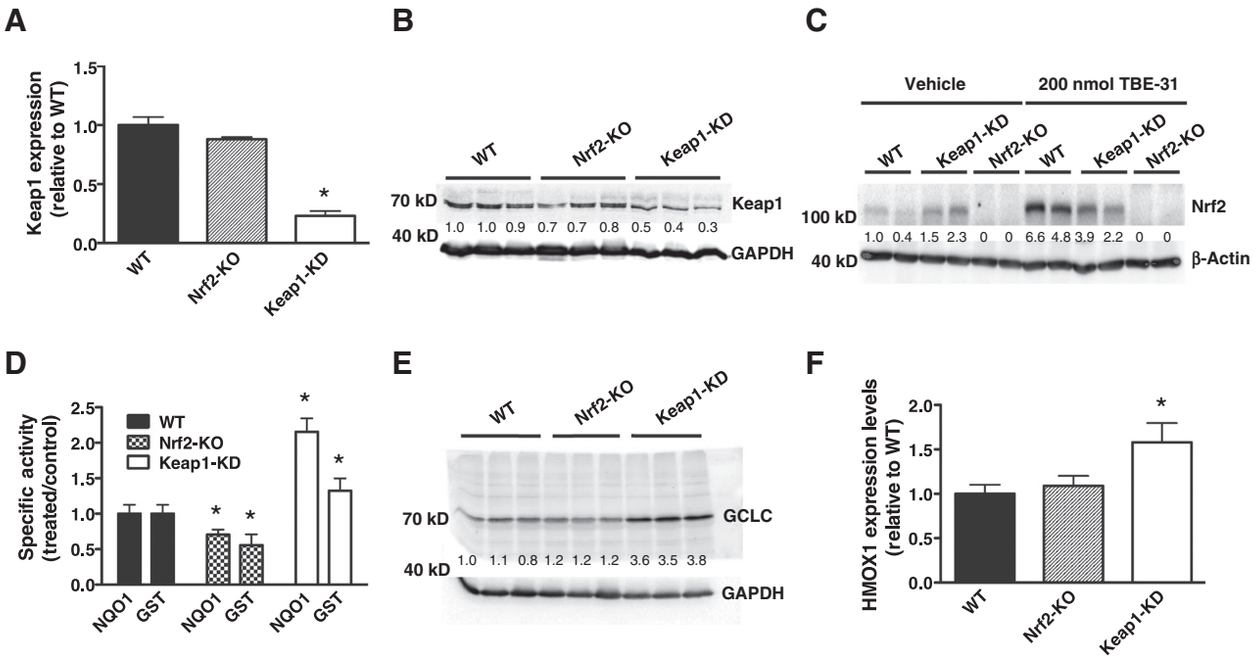

Figure 1.

Genetic upregulation of Nrf2 in the skin of SKH-1 hairless mice leads to enhanced expression of Nrf2 target genes. Quantitative real-time PCR analysis of mRNA (A) and representative immunoblots ($n = 3$; B) of Keap1 from skin samples of WT, Nrf2-KO, and Keap1-KD SKH-1 hairless mice ($n = 3$). C, representative immunoblots ($n = 3$) of Nrf2 levels in skin of vehicle (80% acetone)- or TBE-31 (five daily doses of 200 nmol per mouse, every 24 hours)-treated WT, Keap1-KD and Nrf2-KO SKH-1 hairless mice. D–F, cutaneous NQO1 (menadione as a substrate) and GST (CDNB as a substrate) specific activity (D), GCLC protein levels (E), and HMOX1 mRNA levels (F) in WT, Nrf2-KO, and Keap1-KD SKH-1 hairless mice ($n = 3$). Data were normalized with respect to WT levels. Results are means ± SD. *, $P < 0.001$ for comparisons between WT and mutant skin. The numbers shown in the Western blot analyses represent the ratio of the intensity of each band to that of the corresponding loading control, normalized to one of the wild-type samples.

catalyzes the rate-limiting step in glutathione biosynthesis, are not vastly different between Nrf2-KO and WT skin; however, they are about 3.6-fold higher in the skin of Keap1-KD mice (Fig. 1E). The mRNA levels for heme oxygenase 1 (HMOX1) do not differ significantly between skin samples of Nrf2-KO and WT mice but are 1.6-fold higher ($P < 0.05$) in the skin of Keap1-KD mice (Fig. 1F).

The relatively modest effect of the absence of functional Nrf2 on target gene expression is surprising. It suggests that skin cells may have adapted alternate antioxidant response mechanisms which help them to maintain homeostasis in the face of environmental stresses. Two possible candidates to compensate for the lack of Nrf2 function are Nrf1 and Nrf3, members of the same family of cap'n'collar basic-region leucine zipper transcription factors. Quantitative real-time PCR analysis showed that while the mRNA levels for Nrf1 were not significantly different among the genotypes (Supplementary Fig. S2A), the mRNA levels for Nrf3 were indeed upregulated (by 1.5-fold, $P < 0.001$) compared with WT in skin samples of Nrf2-KO mice (Supplementary Fig. S2B). This finding is in full agreement with the previously reported upregulation of Nrf3 in the skin of Nrf2-knockout mice of a different (mixed) genetic background (30).

Next, we tested the ability of TBE-31 (Fig. 2A), one of the most potent Nrf2 activators known to date (21, 31), to stabilize Nrf2 and induce target gene expression in the skin of mice of the three genotypes. Five daily topical applications of TBE-31 (200 nmol per mouse, 24 hours apart) led to a robust stabilization of Nrf2 in the skin of WT mice (Fig. 1C). This response was diminished in Keap1-KD animals and completely absent in Nrf2-deficient mice, confirming that the Keap1/Nrf2 pathway is the primary target for this compound. In the skin of WT mice, the mRNA levels for the Nrf2 target enzymes NQO1, GCLC, and GSTP were upregulated by 8-, 1.8-, and 1.9-fold, respectively ($P < 0.001$; Fig. 2B). In close agreement, the cutaneous NQO1- and GST-specific enzyme activities were elevated by 6-fold ($P < 0.01$) and 1.8-fold ($P < 0.01$), respectively, 24 hours after the last treatment with TBE-31 (Fig. 2C). In contrast to WT, no induction of NQO1 by TBE-31 was seen in skin of Nrf2-KO mice (Supplementary Fig. S3A). Importantly, induction was not limited to the epidermis (6.9-fold; $P < 0.001$), as it was clearly observed in the dermis, albeit to a smaller (2.5-fold; $P < 0.001$) degree (Supplementary Fig. S3B).

Having established the effect of the Nrf2 status on both basal and inducible expression of its classical target genes in the mouse skin, we then exposed WT mice to a single acute dose of solar-simulated UV radiation and observed dose-dependent changes in the appearance of the skin vasculature 24 hours after exposure (Fig. 3A). We used UV radiation sources with properties nearly identical to the UV component of the sunlight that reaches the surface of the Earth, comprising 5% UVB and 95% UVA wavelengths (Supplementary Fig. S1). The gene expression of the proinflammatory cytokine IL6 was dramatically and dose dependently induced by 16-, 129-, and 170-fold ($P < 0.001$) 24 hours after solar-simulated UV radiation delivering 200, 400, and 600 mJ/cm^2 of UVB, respectively (Fig. 3B). The onset of skin inflammation was further confirmed by the dose-dependent upregulation of IL1β, the levels of which increased by 3-, 16-, and 15-fold

Published OnlineFirst March 24, 2015; DOI: 10.1158/1940-6207.CAPR-14-0362

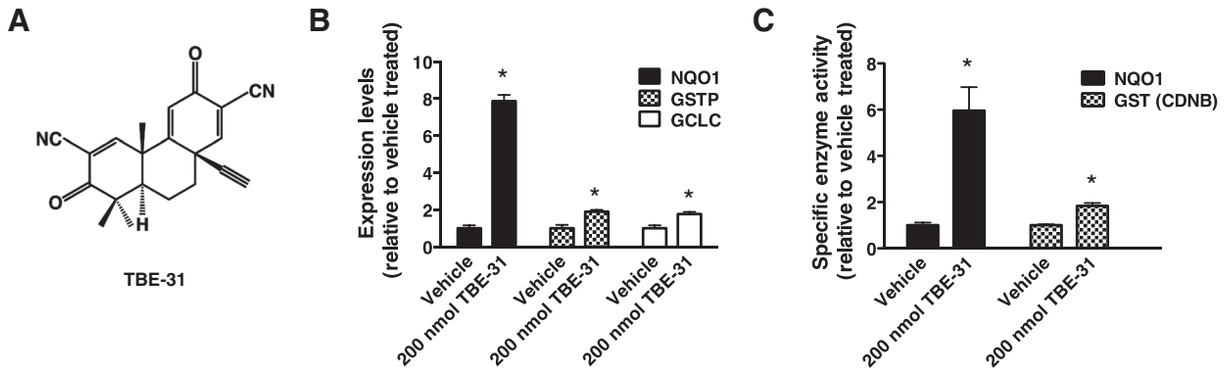

Figure 2.

Pharmacologic upregulation of Nrf2 in the skin of SKH-1 hairless mice leads to enhanced expression of Nrf2 target genes. A, chemical structure of TBE-31. B and C, quantitative real-time PCR analysis of mRNA of NQO1, GSTP, and GCLC (B) and NQO1- (menadione as a substrate) and GST (CDNB as a substrate)-specific activity (C) in skin samples of vehicle (80% acetone)- or TBE-31 (five daily doses of 200 nmol per mouse, every 24 hours, applied topically over the entire back of the animals)-treated WT SKH-1 hairless mice, $n = 3$. Data were normalized with respect to vehicle-treated levels. Results are means ± SD. *, $P < 0.001$ for comparisons between vehicle- and TBE-treated skin.

($P < 0.05$; Fig. 3C). Comparison of the UV radiation–provoked inflammatory responses among mice from the three genotypes revealed that disruption of Nrf2 did not lead to appreciable differences in comparison with WT, but its constitutive upregulation significantly suppressed the production of both proinflammatory cytokines. Thus, compared with WT, 24 hours after irradiation, the upregulation of IL6 and IL1β was reduced by 74- ($P < 0.01$) and 48% ($P < 0.05$), respectively, in the skin of Keap1-KD mice (Fig. 3D and E). Analysis of cellular infiltrates from the affected skin areas showed no significant difference in the total amount of recruited $CD45^+$ cells between WT and Keap1-KD animals (Supplementary Fig. S4). Of note, there was a slight indication of attenuated $CD11b^+Gr1^+$ cells recruitment in the skin of Keap1-KD mice, suggesting reduced neutrophil presence; however, this did not reach statistical significance. Remarkably, 72 hours after exposure to solar-simulated UV radiation, when erythema development was most obvious, the skin of the Keap1-KD animals showed no apparent erythema, in sharp contrast with the skin of their WT and Nrf2-KO counterparts (Fig. 3F). There were no apparent differences in the skin of mutant mice, including epidermal thickness, and the skin architecture of animals of all genotypes appeared very similar and histologically normal (Supplementary Fig. S5). Together, these results demonstrate the protective role of genetic upregulation of Nrf2 against inflammation caused by solar-simulated UV radiation.

Genetic upregulation of Nrf2 protects against skin carcinogenesis caused by solar-simulated UV radiation

The critical role of inflammation for all stages of tumor development is well-established (32). In particular, IL6 is one of the best-characterized protumorigenic cytokines and has been recently proposed to be a new target for cancer therapy (33). As Keap1-KD mice showed a very substantial reduction in induction of IL6 expression provoked by solar-simulated UV radiation (Fig. 3D) and they also express higher levels of cytoprotective enzymes in their skin (Fig. 1D–F) than their WT or Nrf2-KO counterparts, we hypothesized that Keap1-KD mice will be protected against skin carcinogenesis in comparison with WT or Nrf2-KO animals. Conversely, because Nrf2-KO were not substantially different from WT mice in terms of inflammatory responses to solar-simulated UV radiation (Fig. 3D–F), they were expected not to be significantly different from WT with respect to development of skin tumors. To test this hypothesis, we subjected groups of 30 mice of each of the three genotypes to chronic exposure to suberythemal doses of solar-simulated UV radiation (comprised of 2 J/cm^2 UVA and 90 mJ/cm^2 UVB), twice a week for 15 weeks. Tumor development was then followed during the subsequent 20 weeks. Notably, the histopathologic spectrum of the tumors which form in this mouse model closely resembles the spectrum of human cSCC, including well- and moderately differentiated tumors (Fig. 4A).

In agreement with the lack of profound differences in expression of Nrf2 downstream target genes (Fig. 1D–F) and solar-simulated UV radiation–mediated induction in proinflammatory cytokines (Fig. 3D and E) between Nrf2-KO and WT mice, there were no significant differences in tumor incidence, multiplicity, or burden between these two genotypes (Fig. 4B–D). In sharp contrast, the Keap1-KD mice were substantially protected against the carcinogenic effects of solar-simulated UV radiation. Thus, whereas 50% of WT and Nrf2-KO mice had tumors at treatment week 24 (i.e., 9 weeks after the UV radiation schedule was discontinued), it took nearly twice as long (i.e., 16 weeks or treatment week 30) for 50% of the Keap1-KD mice to develop their first tumor (Fig. 4B). At the end of the experiment, more than 90% of the WT and Nrf2-KO animals had tumors, whereas tumor incidence was 60% in the Keap1-KD mice. Kaplan–Meier "survival analysis" applied to freedom-from-tumors, followed by a log-rank test for equality of survivor function showed a highly significant difference between the Keap1-KD and the WT groups ($\chi^2 = 25.9$; $P < 0.0001$). The effect of genetic Nrf2 upregulation on tumor multiplicity was even more profound, and there was a ∼5-fold reduction, from 5.4 tumors per mouse in the WT group to 1 tumor per mouse in the Keap1-KD group (Fig. 4C). The difference between groups was highly significant by ANOVA followed by Bartlett test for equal variances ($F = 80.18$, $P < 0.0001$) and even stronger for comparison of just the Keap1-KD group with the WT group ($F = 157.59$, $P < 0.0001$). The Keap1-KD group became significantly different from the WT group by week 23. The total tumor volume (expressed in mm^3) per mouse was also profoundly affected by the genetic upregulation of Nrf2 (Fig. 4D), and there was a significant 80% reduction between the Keap1-KD and the

Published OnlineFirst March 24, 2015; DOI: 10.1158/1940-6207.CAPR-14-0362

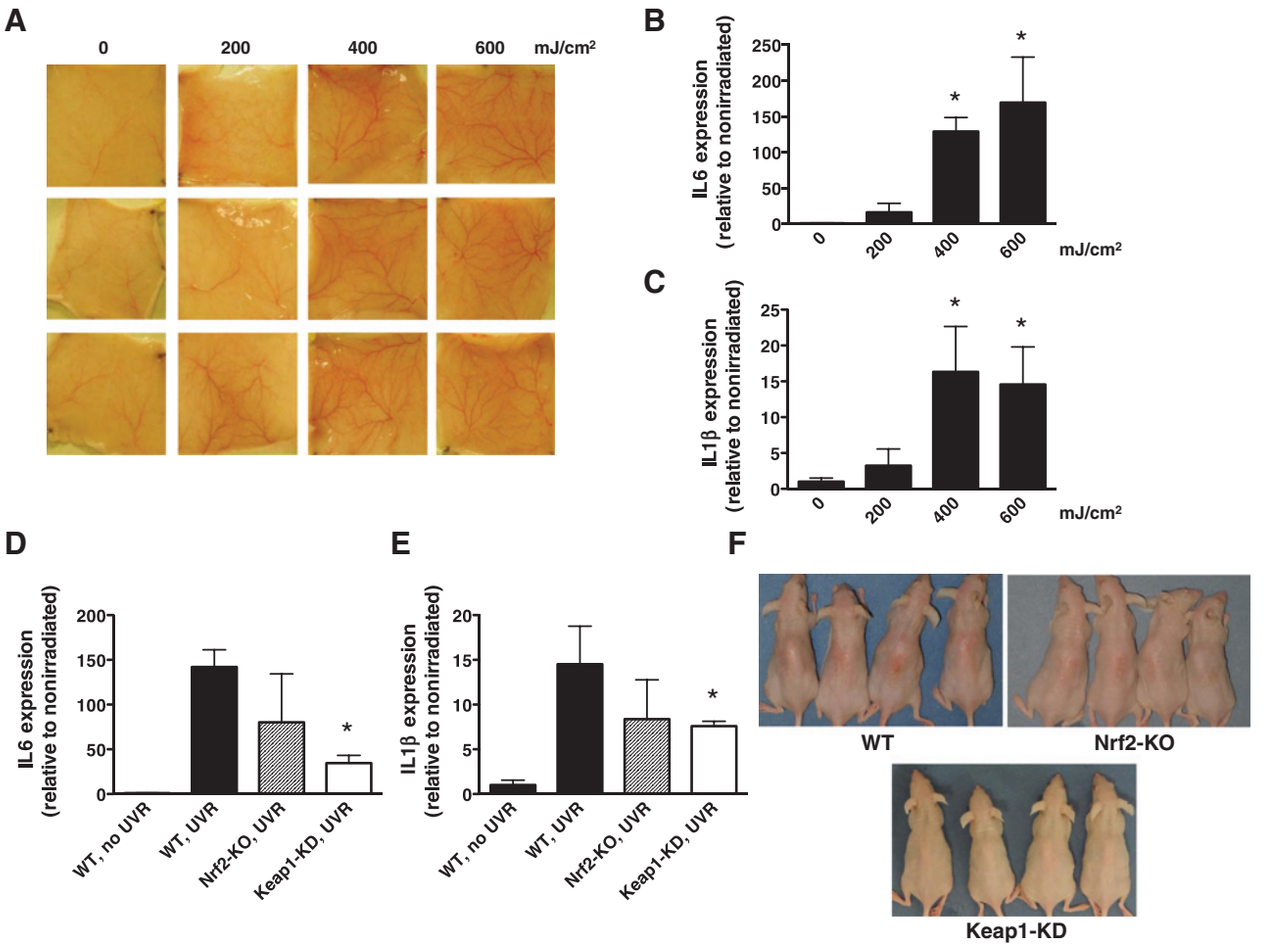

Figure 3.
Genetic upregulation of Nrf2 in the skin of SKH-1 hairless mice protects against inflammation caused by solar-simulated UV radiation. A, images of the dorsal skin vasculature of 12 individual animals (4 groups of 3, arranged in columns) used for analyses of the inflammatory markers shown in B and C. Quantitative real-time PCR analysis of cutaneous mRNA levels of IL6 (B) and IL1β (C) of WT SKH-1 hairless mice ($n = 3$) 24 hours after acute exposure to a single dose (the indicated doses refer to the UVB component) of solar-simulated UV radiation. Quantitative real-time PCR analysis of mRNA of IL6 (D) and IL1β (E) in skin samples of WT, Nrf2-KO, and Keap1-KD SKH-1 hairless mice ($n = 3$) 24 hours after acute exposure to a single dose (UVB component = 400 mJ/cm^2) of solar-simulated UV radiation. Data were normalized with respect to levels in nonirradiated skin. Results are means ± SD. *, $P < 0.05$. F, photographs of WT, Nrf2-KO, and Keap1-KD SKH-1 hairless mice showing delayed erythemal response 72 hours after irradiation.

WT groups over the last 3 weeks of the experiment (i.e., weeks 33–35; $F = 9.36$, $P < 0.0022$).

Pharmacologic activation of Nrf2 protects against inflammation caused by solar-simulated UV radiation

To test whether similar to genetic, pharmacologic Nrf2 activation can also protect against solar-simulated UV radiation-mediated inflammation, we used TBE-31. At low nanomolar concentrations, this acetylenic tricyclic bis(cyano enone) compound induces cytoprotective enzymes and inhibits IFNγ-mediated proinflammatory responses (21, 31, 34). Three daily topical applications of 40 nmol of TBE-31, every 24 hours, did not affect the expression of IL6, IL1β, or prostaglandin-endoperoxide synthase (more commonly known as COX2) in nonirradiated murine skin (Fig. 5A–C). However, after exposure to solar-simulated UV radiation, the mRNA levels for the 3 inflammatory markers were lower in the skin of TBE-31- than in vehicle-treated mice (Fig. 5D–F). Thus, compared with vehicle treatment, 24 hours after irradiation, the upregulation of IL6, IL1β, and COX2 was decreased by 55- ($P < 0.001$), 24- ($P < 0.05$), and 30% ($P < 0.05$), respectively, in the skin of TBE-31–treated mice. The protective effect of TBE-31 against UV radiation–induced inflammation was largely absent in Nrf2-KO mice (Fig. 5G–I), although there was an apparent nonstatistically significant protection against IL1β upregulation in the skin of Nrf2-KO mice (Fig. 5H), in agreement with our previous report that some, but not all of the anti-inflammatory effects of compounds of this type are Nrf2-dependent (35).

Pharmacologic activation of Nrf2 protects against skin carcinogenesis caused by solar-simulated UV radiation during azathioprine treatment

Azathioprine is a highly effective anti-inflammatory and immunosuppressive agent that is widely used for the treatment of

Published OnlineFirst March 24, 2015; DOI: 10.1158/1940-6207.CAPR-14-0362

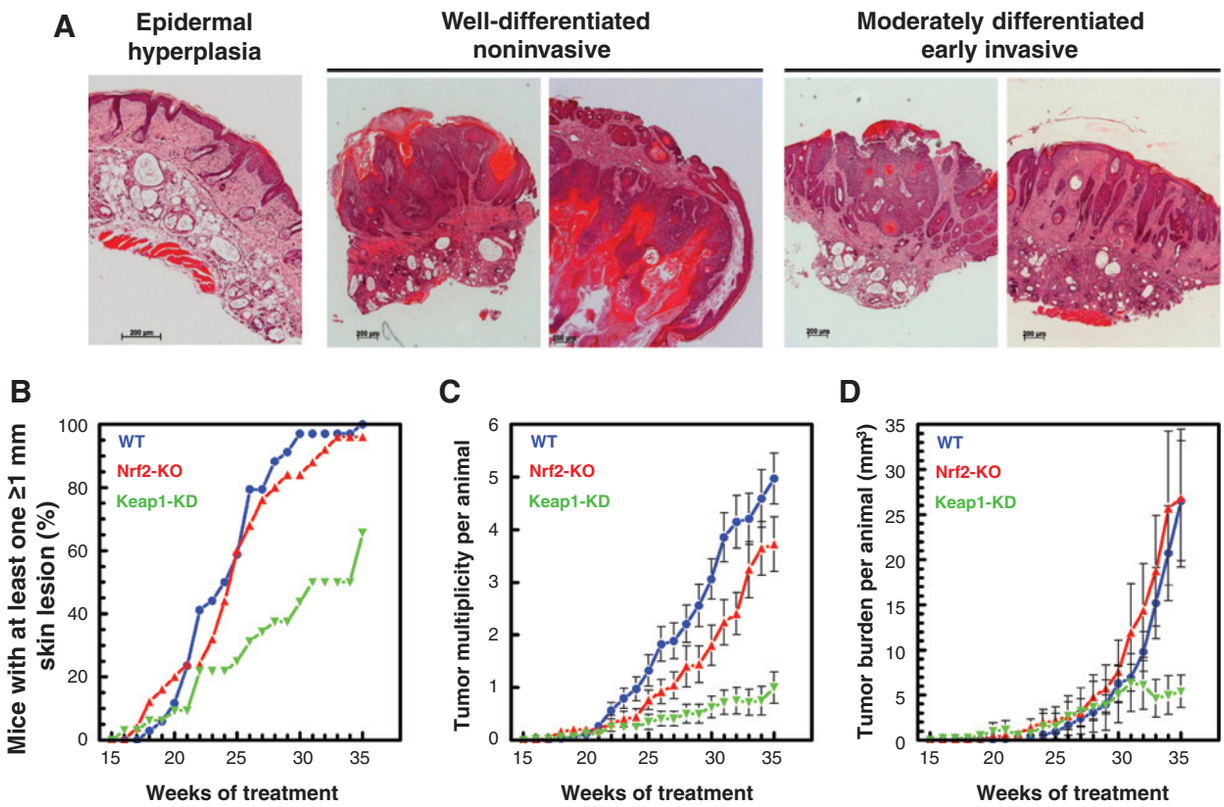

Figure 4.

Genetic upregulation of Nrf2 protects against cutaneous carcinogenesis mediated by solar-simulated UV radiation. A, histopathology of tumors which form after chronic exposure to solar-simulated UV radiation in SKH-1 hairless mice. Examples are shown of epithelial lesions, including premalignant epidermal hyperplasia, well-differentiated noninvasive, and moderately differentiated early-invasive cSCC. Scale bar, 200 μm. B–D, WT, Nrf2-KO, and Keap1-KD SKH-1 hairless mice ($n = 30$, with every cage housing representatives of each genotype) were exposed chronically to solar-simulated UV radiation (composed of 2 J/cm^2 UVA and 90 mJ/cm^2 UVB), twice a week for 15 weeks. During the subsequent 20 weeks, the appearance of tumors was monitored weekly, the lesions were mapped, counted, and their volumes determined. The number of tumors per mouse (multiplicity) and the tumor burden are expressed as average values ± SEM based on the total number of animals at risk.

inflammatory bowel disease and in solid organ transplantation. Its active metabolite, 6-thioguanine (6-TG) incorporates in genomic DNA during replication. The combination of 6-TG and UVA radiation is highly mutagenic and increases the sensitivity of the human skin to UVA radiation (36). 6-TG is a UVA photosensitizer, leading to formation of ROS which cause oxidative damage to DNA and proteins, including DNA damage repair enzymes, thus compromising DNA break rejoining and base and nucleotide excision repair (37). These findings have provided a direct causative link between thiopurine therapies and the associated increased (by more than 100-fold relative to the general population) risk for highly aggressive cSCC.

To test whether activation of Nrf2 can protect against solar-simulated UV radiation–mediated skin carcinogenesis under conditions of azathioprine therapy, we used a pharmacologic approach. We have previously shown that TBE-31, at low nanomolar concentrations, protects cultured murine keratinocytes (Kera-308 cells) against generation of ROS after exposure to 6-TG (a surrogate for azathioprine) and UVA radiation (38). Importantly, the protective effect of TBE-31 correlated with a robust upregulation of the activities of the Nrf2 target enzymes NQO1 and GST. Because ROS are important mediators of the mutagenic effects of the combination of 6-TG and UV radiation (39), and TBE-31 effectively reduced inflammation in mice exposed to solar-simulated UV radiation (Fig. 5), together these data suggest that TBE-31 is a good candidate for a pharmacologic protective agent against UV radiation–mediated skin carcinogenesis under conditions of azathioprine therapy.

On the basis of detailed pharmacokinetics and dose optimization experiments (Supplementary Results and Supplementary Figs. S6 and S7), we began administering TBE-31 (40 nmol/mouse/d, topically, 2 d/wk) simultaneously with azathioprine (1 mg/kg/d in the drinking water) 2 weeks before the start of the irradiation schedule and continued applying both TBE-31 and azathioprine at this dosing regimen throughout the duration of the experiment (a total of 33 weeks). Similar to the experiment with the three genotypes of mice, the animals were exposed to chronic suberythemal solar-simulated UV radiation (comprised of 2 J/cm^2 UVA and 90 mJ/cm^2 UVB). Notably, these solar-simulated UV radiation sources have a peak emission at 340 nm (Supplementary Fig. S1), which coincides with the absorption peak of 6-TG, the active metabolite of azathioprine (39). After biweekly exposures for 15 weeks, irradiation was discontinued, and tumor development was evaluated during the subsequent 16 weeks.

Published OnlineFirst March 24, 2015; DOI: 10.1158/1940-6207.CAPR-14-0362

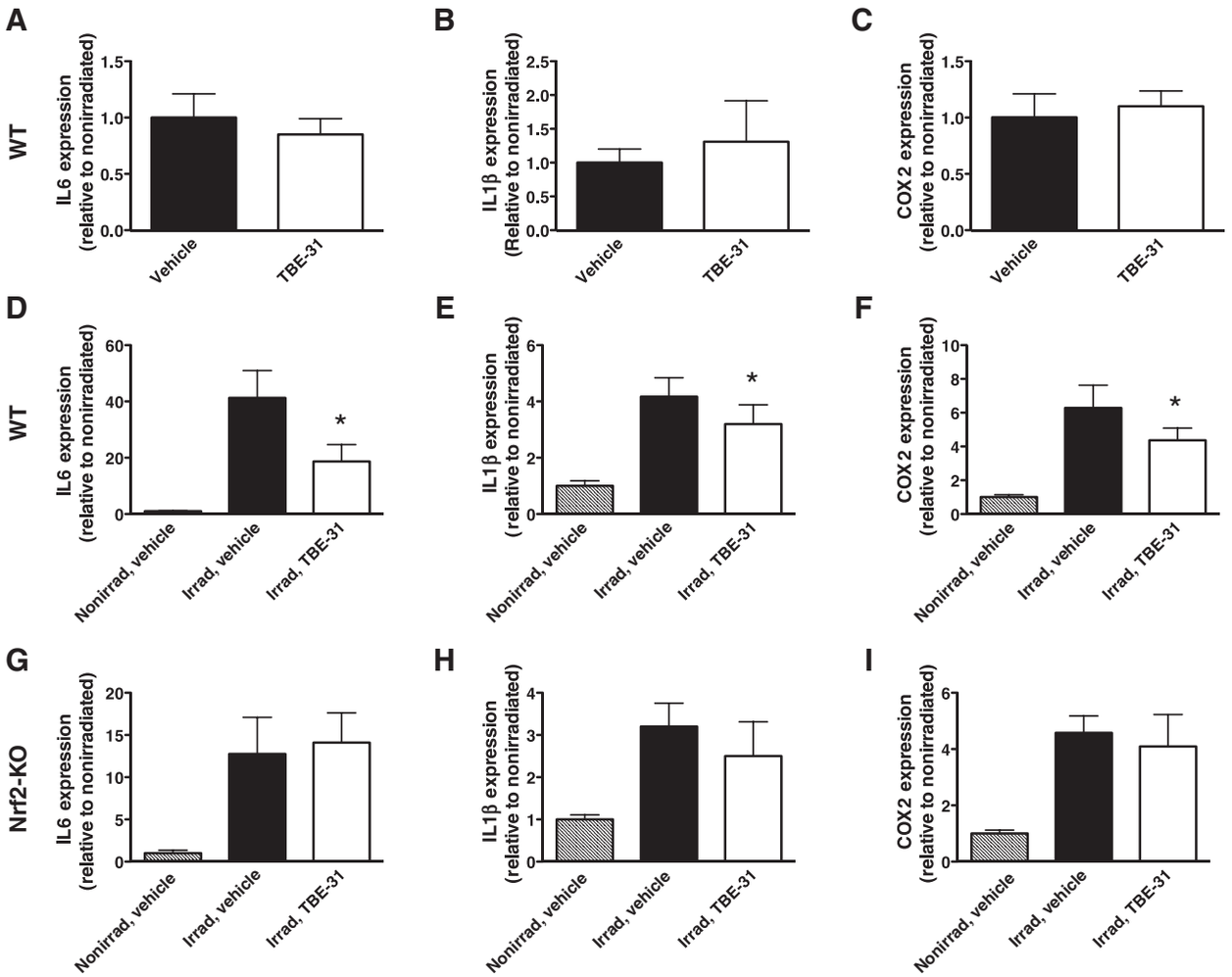

Figure 5.
Pharmacologic upregulation of Nrf2 in the skin of SKH-1 hairless mice protects against inflammation caused by solar-simulated UV radiation. Quantitative real-time PCR analysis of mRNA of IL6 (A, D, G), IL1β (B, E, H), and COX2 (C, F, I) in skin samples of nonirradiated WT SKH-1 hairless mice (A–C) or WT (D–F) and Nrf2-KO (G–I) animals 24 hours after acute exposure to a single dose (UVB component = 400 mJ/cm^2) of solar-simulated UV radiation. Two groups of each genotype of mice ($n = 5$) were used. The first one was treated with vehicle (80% acetone), whereas the second one received TBE-31 (3 daily doses of 40 nmol per mouse, every 24 hours, applied topically). Data were normalized with respect to levels in vehicle-treated nonirradiated skin. Results are means ± SD. *, $P < 0.05$ for comparison between irradiated vehicle-treated and irradiated TBE-31–treated animals.

Whereas tumor incidence was not significantly different between the control and the TBE-31–treated groups (Fig. 6A), TBE-31 significantly reduced tumor multiplicity (Fig. 6B). Kaplan–Meier survival analysis applied to freedom-from-tumors, followed by a log-rank test for equality of survivor function showed no significant difference between groups. However, the differences in average tumor number were highly significant ($F = 39.11$, $P < 0.0001$) by one-way ANOVA followed by Bartlett test for equal variances, with the control group ultimately having 9.5 tumors per mouse, compared with 5.3 tumors per mouse for the TBE-treated group; differences in tumor number became significant at week 23. Moreover, the protective effect of TBE-31 was especially striking with respect to tumor volume, which was markedly reduced (~5-fold), from 225 mm^3 per mouse in the vehicle-treated group to 41.9 mm^3 in the TBE-31–treated group (Fig. 6C). The difference between the groups was highly significant ($F = 18.16$, $P < 0.0001$) by one-way ANOVA followed by Bartlett test for equal variances.

Topical application of extracts containing the Nrf2 activator sulforaphane protects healthy human subjects against skin erythema development caused by solar-simulated UV radiation

In a proof-of-principle study with 6 healthy human subjects, we have previously shown that, compared with vehicle-treated sites, the intensity of narrow-band (311 nm) UVB radiation–induced skin erythema was reduced by around 40% at sites that received topical treatment with broccoli extracts delivering the naturally occurring Nrf2 activator sulforaphane (15). As TBE-31 is a synthetic compound which has not yet been approved for use in humans, we used sulforaphane-rich broccoli extracts to test the hypothesis that, as in mice, pharmacologic activation of Nrf2 will protect humans against skin damage by solar-simulated UV radiation. Skin erythema was used as a quantifiable

Published OnlineFirst March 24, 2015; DOI: 10.1158/1940-6207.CAPR-14-0362

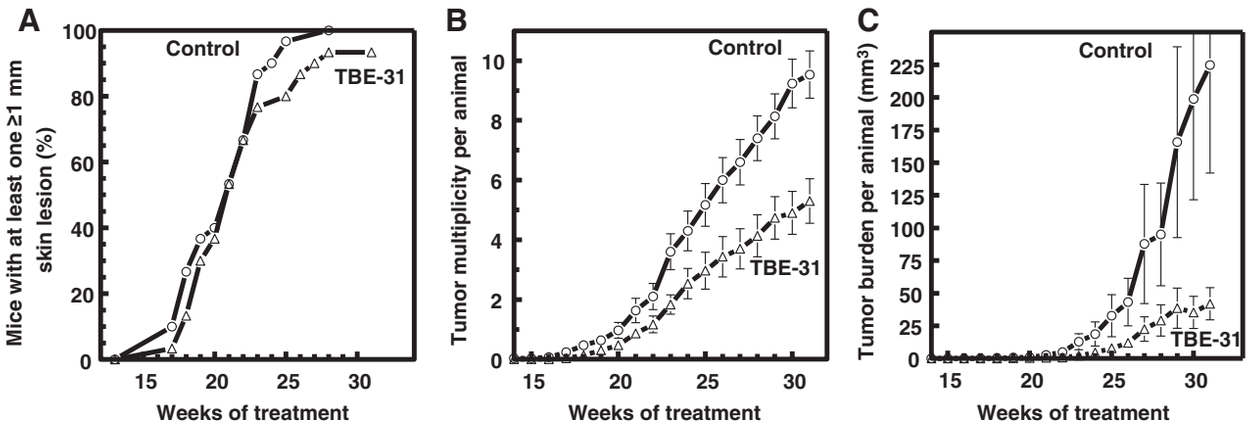

Figure 6.
Pharmacologic upregulation of Nrf2 by TBE-31 protects against cutaneous carcinogenesis mediated by solar-simulated UV radiation in mice receiving azathioprine therapy. WT SKH-1 hairless mice ($n = 30$) were treated with azathioprine (1 mg/kg/d, orally, dissolved in the drinking water) and either vehicle (80% acetone) or TBE-31 (40 nmol per mouse, twice a week, topically, in 200 μL of 80% acetone). Two weeks after beginning of treatment with azathioprine and TBE-31, the animals were exposed chronically to solar-simulated UV radiation (composed of 2 J/cm^2 UVA and 90 mJ/cm^2 UVB), twice a week for a further 15 weeks. Irradiation was then stopped, but treatment with both azathioprine and TBE-31 was continued for the duration of the experiment. During the subsequent 16 weeks, the appearance of tumors was monitored weekly, the lesions were mapped, counted, and their volumes determined. The graphs show tumor incidence (A), multiplicity (B), and burden (C). The number of tumors per mouse (multiplicity) and the tumor volume are expressed as average values ± SEM based on the total number of animals at risk.

surrogate endpoint for cutaneous damage and skin cancer risk (40).

The study was randomized, double-blind, and placebo-controlled (Fig. 7A). We compared the response of the skin of 24 healthy human volunteers, men and women, to different wavebands of monochromator UV radiation and solar-simulated UV waveband radiation after topical application of extracts containing either sulforaphane (SF, active) or the inactive precursor of sulforaphane, glucoraphanin (GR, placebo; Supplementary Figs. S8 and S9), in a double-blind side-by-side comparison, with each subject acting as his/her own control. We applied in a randomized fashion to the right or the left half of the mid-upper back skin (avoiding the paravertebral area) of each volunteer either active or placebo extract containing 200 nmol/cm^2 of sulforaphane or glucoraphanin, respectively, 3 times, 24 hours apart. The choice of this dose was based on our previous studies in which we showed that sulforaphane caused a dose-dependent induction of NQO1 in human skin punch biopsies (41). The study was conducted on an outpatient basis because prior experience had indicated no significant adverse reactions of the human skin to application of these doses of the extracts. Twenty-four hours after the last extract applications, small areas of the skin (~1 cm^2) within the extract-treated areas were exposed to a range of doses of monochromatic UV radiation and visible light, and solar-

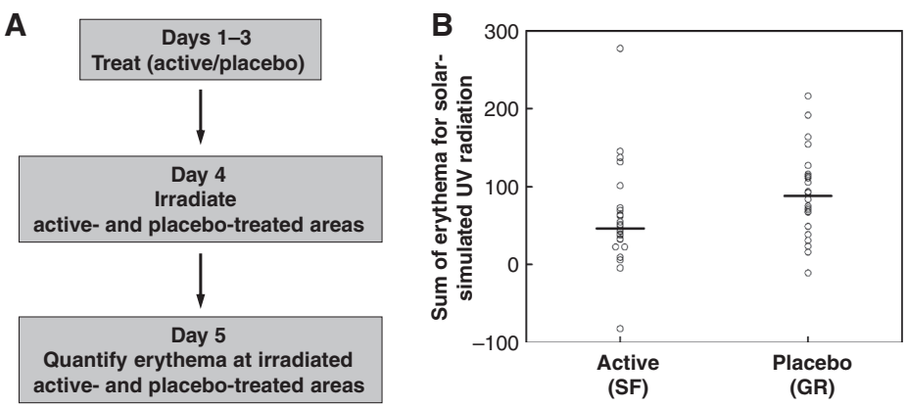

Figure 7.
Topical application of extracts containing the Nrf2 activator sulforaphane reduces the degree of skin erythema following acute exposure to solar-simulated UV radiation in healthy human subjects. A, study design. Twenty-four healthy human subjects received topically, on their upper back, two types of plant extracts: sulforaphane-rich (SF, active), and glucoraphanin-rich (GR, placebo), 3 times, 24 hours apart. One day after the last extract application, small areas (~1 cm^2) of skin were exposed to a range of doses of solar simulated UV radiation. Erythema was determined 24 hours later semiquantitatively by naked eye and quantified objectively using an erythema meter. B, sum of erythema for all doses of solar-simulated UV radiation. Data are presented as the average of 3 independent measurements for the irradiated sites minus the average of 3 measurements for nonirradiated (background) sites. The difference between placebo- and active extract–treated sites is statistically significant ($P = 0.02$).

Published OnlineFirst March 24, 2015; DOI: 10.1158/1940-6207.CAPR-14-0362

simulated UV radiation according to a standardized solar simulator phototesting technique that is used routinely in the Photobiology Unit at Ninewells Hospital (Dundee, Scotland, UK; ref. 42). Skin responses to each dose of radiation were assessed 24 hours after irradiation by using a semiquantitative visual scale and quantifying objectively the resulting erythema using an erythema meter. Critically, those making the erythema measurements were blinded to treatment, allowing for an unbiased objective comparison of the degrees of erythemal response between active- and placebo-treated areas.

Because we used a series of radiation doses for each subject, we calculated the sum of erythema, rather than simply taking the intensity of erythema at 24 hours after a particular dose. This process takes into account individual differences in erythemal sensitivity in terms of both the threshold and slope of response. No significant differences in threshold responses, that is, MED, were observed at any of the wavelengths. However, mean erythema sum after testing with one of the wavebands (the solar simulator) for the placebo-treated sites was 91, compared with 59 for the active-treated sites, a difference in mean erythema of 31 (95% confidence interval, 6–58; $P = 0.02$; Fig. 7B). Thus, compared with placebo-treated areas of the skin, the overall erythemal response was reduced by 35% at areas that had received the pharmacologic Nrf2 activator.

Discussion

Exome sequencing of human primary cSCC and matched normal tissue has revealed an extraordinary large mutation burden of approximately 1,300 somatic single-nucleotide variants per exome (13), making the possibility for success of a single-target therapy unlikely and highlighting the need for agents capable of affecting multiple hallmarks of cancer. Nrf2-dependent cytoprotective responses provide broad, versatile, and long-lasting protection that counteracts many of the damaging effects of solar UV radiation, a complete carcinogen which can cause the initiation, promotion, and progression of cSCC. Because of its crucial role in cytoprotection, including regulation of the cellular redox homeostasis, Nrf2 is now considered a drug target (43). However, the frequent activation of Nrf2 in established human tumors has raised the critical question whether Nrf2 may also be a driver in cancer.

Using the oncogenic H-Ras(Q61L)-driven DMBA/TPA model, it has been shown that skin carcinogenesis is enhanced in mice which are either deficient for Nrf2 (16) or express a dominant-negative form of Nrf2 in the epidermis (44). This mutant H-Ras–driven chemical carcinogenesis model gives rise primarily to benign papillomas and is very different from the solar UV radiation–induced cSCC, in which H-Ras mutations are rare (45). By generating SKH-1 hairless mice in which Nrf2 is either disrupted (Nrf2-KO SKH-1 hairless) or constitutively upregulated (Keap1-KD SKH-1 hairless), and using chronic twice-weekly exposures to solar-simulated UV radiation as the carcinogen, we addressed the role of Nrf2 in solar UV radiation–induced skin carcinogenesis. To our knowledge, Keap1-KD mice on any genetic background have not been previously used in any carcinogenesis model. Importantly, the extent of activation of Nrf2 in both models (genetic and pharmacologic) described in this contribution does not cause any obvious skin abnormalities (Supplementary Fig. S5) and furthermore is comparable to the level of pharmacologic Nrf2 activation which is achievable in the human skin (41). This is in contrast to the very high levels of Nrf2 activity that are seen in the skin of mice genetically engineered to express keratinocyte-specific constitutively active mutant Nrf2 under the control of a β-actin promoter and a CMV enhancer, the expression of which causes sebaceous gland hypertrophy, hyperkeratosis, and cyst formation (46). We found that genetic or pharmacologic activation of Nrf2 results in higher expression of cytoprotective enzymes, suppression of UV radiation–evoked proinflammatory responses, and marked reduction in tumor growth. Importantly, the protective effect of Nrf2 activation is evident in both immunocompetent mice as well as in animals that are receiving life-long treatment with the immunosuppressive agent azathioprine. This finding indicates that pharmacologic activation of Nrf2 could be an effective strategy for protection against cSCC in both the general population and high-risk groups, such as patients with organ transplant recipients and inflammatory bowel disease, and encourage the clinical development of potent and specific Nrf2 activators, such as TBE-31. This conclusion is further strengthened by the fact that in healthy human subjects, pharmacologic activation of Nrf2 is protective against solar-simulated UV radiation–evoked erythema, a surrogate marker for cutaneous photodamage and skin cancer risk (40).

It was recently demonstrated that Nrf2 directs carbon flux toward the pentose phosphate pathway and the tricarboxylic acid cycle, and furthermore, during sustained activation of PI3K/Akt signaling, this transcription factor redirects glucose and glutamine into anabolic pathways (47, 48). In addition, it has been shown that following expression of endogenous oncogenic alleles of K-Ras, B-Raf, and Myc, transcription of Nrf2 is increased, whereas the number of neoplastic cells in the pancreas produced by transgenic expression of oncogenic K-Ras(G12D) and their proliferation rate are decreased in Nrf2-KO mice in comparison with their WT counterparts (49). Curiously, dietary supplementation with the antioxidants *N*-acetylcysteine or vitamin E accelerates tumor progression and decreases survival in mouse models of oncogenic B-Raf- and K-Ras–induced lung cancer, and RNA sequencing has revealed changes in tumor transcriptome profiles that are characterized by reduced expression of Nrf2-dependent antioxidant genes (50). Together with these findings, the results from the present study imply that Nrf2 is not a driver for skin carcinogenesis and strongly suggest that this is very likely also to be the case for other malignancies. Rather, the frequent activation of Nrf2 that is seen in many established human tumors is a marker of metabolic adaptation that allows growth and survival under conditions of disrupted metabolic balance and compromised redox and energy homeostasis.

Disclosure of Potential Conflicts of Interest

No potential conflicts of interest were disclosed.

Authors' Contributions

Conception and design: E.V. Knatko, S.H. Ibbotson, P. Talalay, A.L. Benedict, T. Honda, C.M. Proby, A.T. Dinkova-Kostova

Development of methodology: E.V. Knatko, S.H. Ibbotson, J.W. Fahey, P. Talalay, R.S. Dawe, J.T.-J. Huang, R. Clarke, A.T. Dinkova-Kostova

Acquisition of data (provided animals, acquired and managed patients, provided facilities, etc.): E.V. Knatko, S.H. Ibbotson, Y. Zhang, M. Higgins, R. Clarke, S. Zheng, S. Kalra, A.T. Dinkova-Kostova

Analysis and interpretation of data (e.g., statistical analysis, biostatistics, computational analysis): E.V. Knatko, J.W. Fahey, R.S. Dawe, J.T.-J. Huang, R. Clarke, A.T. Dinkova-Kostova

Writing, review, and/or revision of the manuscript: E.V. Knatko, S.H. Ibbotson, Y. Zhang, J.W. Fahey, P. Talalay, R.S. Dawe, J.T.-J. Huang, S. Kalra, A.L. Benedict, T. Honda, C.M. Proby, A.T. Dinkova-Kostova

Administrative, technical, or material support (i.e., reporting or organizing data, constructing databases): M. Higgins, J.W. Fahey, J. Ferguson, J.T.-J. Huang, A. Saito, A.L. Benedict, T. Honda, A.T. Dinkova-Kostova
Study supervision: S.H. Ibbotson, A.T. Dinkova-Kostova
Other (ethical approval for the study and liaison with the Photodermatology department): C.M. Proby

Acknowledgments

The authors thank the healthy volunteers who participated in the human study, the staff of the Photobiology Unit (Ninewells Hospital) for their generous help, and especially to June Gardner, Lynn Fullerton, and Julie Woods. They also thank Sheila Sharp at Biomarker and Drug Analysis Core Facility for providing services in pharmacokinetics analysis, Masayuki Yamamoto (Tohoku University) for the Nrf2-knockout and Keap1-KD C57BL/6 mice that were used to generate the Nrf2-knockout and Keap1-KD SKH-1 hairless mice, and John D. Hayes (University of Dundee) for antibodies and helpful discussions. S. Zheng and A. Saito are grateful to the Institute of Chemical Biology and Drug Discovery for Postdoctoral Scholarships. This article is dedicated to Professor Iwao Ojima, a Distinguished Professor at Stony Brook University, in celebration of his seventieth birthday.

Grant Support

This work was supported by Cancer Research UK (C20953/A10270 to A.T. Dinkova-Kostova), the BBSRC (BB/J007498/1 to A.T. Dinkova-Kostova), Stony Brook Foundation (to T. Honda), and Reata Pharmaceuticals (to T. Honda).

The costs of publication of this article were defrayed in part by the payment of page charges. This article must therefore be hereby marked *advertisement* in accordance with 18 U.S.C. Section 1734 solely to indicate this fact.

Received October 15, 2014; revised February 25, 2015; accepted March 13, 2015; published OnlineFirst March 24, 2015.

References

1. Kensler TW, Wakabayashi N, Biswal S. Cell survival responses to environmental stresses via the Keap1-Nrf2-ARE pathway. Annu Rev Pharmacol Toxicol 2007;47:89–116.
2. Taguchi K, Motohashi H, Yamamoto M. Molecular mechanisms of the Keap1-Nrf2 pathway in stress response and cancer evolution. Genes Cells 2011;16:123–40.
3. Talalay P, Dinkova-Kostova AT, Holtzclaw WD. Importance of phase 2 gene regulation in protection against electrophile and reactive oxygen toxicity and carcinogenesis. Adv Enzyme Regul 2003;43:121–34.
4. Hayes JD, Dinkova-Kostova AT. The Nrf2 regulatory network provides an interface between redox and intermediary metabolism. Trends Biochem Sci 2014;39:199–218.
5. Cullinan SB, Gordan JD, Jin J, Harper JW, Diehl JA. The Keap1-BTB protein is an adaptor that bridges Nrf2 to a Cul3-based E3 ligase: oxidative stress sensing by a Cul3-Keap1 ligase. Mol Cell Biol 2004;24:8477–86.
6. Zhang DD, Lo SC, Cross JV, Templeton DJ, Hannink M. Keap1 is a redox-regulated substrate adaptor protein for a Cul3-dependent ubiquitin ligase complex. Mol Cell Biol 2004;24:10941–53.
7. Kobayashi A, Kang MI, Okawa H, Ohtsuji M, Zenke Y, Chiba T, et al. Oxidative stress sensor Keap1 functions as an adaptor for Cul3-based E3 ligase to regulate proteasomal degradation of Nrf2. Mol Cell Biol 2004;24:7130–9.
8. Dinkova-Kostova AT, Holtzclaw WD, Cole RN, Itoh K, Wakabayashi N, Katoh Y, et al. Direct evidence that sulfhydryl groups of Keap1 are the sensors regulating induction of phase 2 enzymes that protect against carcinogens and oxidants. Proc Natl Acad Sci U S A 2002;99:11908–13.
9. McMahon M, Lamont DJ, Beattie KA, Hayes JD. Keap1 perceives stress via three sensors for the endogenous signaling molecules nitric oxide, zinc, and alkenals. Proc Natl Acad Sci U S A 2010;107:18838–43.
10. Suzuki T, Motohashi H, Yamamoto M. Toward clinical application of the Keap1-Nrf2 pathway. Trends Pharmacol Sci 2013;34:340–6.
11. Jaramillo MC, Zhang DD. The emerging role of the Nrf2-Keap1 signaling pathway in cancer. Genes Dev 2013;27:2179–91.
12. Narayanan DL, Saladi RN, Fox JL. Ultraviolet radiation and skin cancer. Int J Dermatol 2010;49:978–86.
13. Durinck S, Ho C, Wang NJ, Liao W, Jakkula LR, Collisson EA, et al. Temporal dissection of tumorigenesis in primary cancers. Cancer Discov 2011;1:137–43.
14. Harwood CA, Mesher D, McGregor JM, Mitchell L, Leedham-Green M, Raftery M, et al. A surveillance model for skin cancer in organ transplant recipients: a 22-year prospective study in an ethnically diverse population. Am J Transplant 2013;13:119–29.
15. Talalay P, Fahey JW, Healy ZR, Wehage SL, Benedict AL, Min C, et al. Sulforaphane mobilizes cellular defenses that protect skin against damage by UV radiation. Proc Natl Acad Sci U S A 2007;104:17500–5.
16. Xu C, Huang MT, Shen G, Yuan X, Lin W, Khor TO, et al. Inhibition of 7,12-dimethylbenz(a)anthracene-induced skin tumorigenesis in C57BL/6 mice by sulforaphane is mediated by nuclear factor E2-related factor 2. Cancer Res 2006;66:8293–6.
17. Gills JJ, Jeffery EH, Matusheski NV, Moon RC, Lantvit DD, Pezzuto JM. Sulforaphane prevents mouse skin tumorigenesis during the stage of promotion. Cancer Lett 2006;236:72–9.
18. Dinkova-Kostova AT, Jenkins SN, Fahey JW, Ye L, Wehage SL, Liby KT, et al. Protection against UV-light-induced skin carcinogenesis in SKH-1 high-risk mice by sulforaphane-containing broccoli sprout extracts. Cancer Lett 2006;240:243–52.
19. Dinkova-Kostova AT, Fahey JW, Benedict AL, Jenkins SN, Ye L, Wehage SL, et al. Dietary glucoraphanin-rich broccoli sprout extracts protect against UV radiation-induced skin carcinogenesis in SKH-1 hairless mice. Photochem Photobiol Sci 2010;9:597–600.
20. Benavides F, Oberyszyn TM, VanBuskirk AM, Reeve VE, Kusewitt DF. The hairless mouse in skin research. J Dermatol Sci 2009;53:10–8.
21. Honda T, Yoshizawa H, Sundararajan C, David E, Lajoie MJ, Favaloro FG Jr, et al. Tricyclic compounds containing nonenolizable cyano enones. A novel class of highly potent anti-inflammatory and cytoprotective agents. J Med Chem 2011;54:1762–78.
22. Saito A, Zheng S, Takahashi M, Li W, Ojima I, Honda T. An improved synthesis of a hydroxymethyl tricyclicketone from cyclohexanone, the key process for the synthesis of a highly potent anti-inflammatory and cytoprotective agent. Synthesis 2013;45:3251–4.
23. Zheng S, Huang JT, Knatko EV, Sharp S, Higgins M, Ojima I, et al. Synthesis of $^{13}C_2$ $^{15}N_2$-labeled anti-inflammatory and cytoprotective tricyclic *bis* (cyanoenone) ([$^{13}C_2$ $^{15}N_2$]-TBE-31) as an internal standard for quantification by stable isotope dilution LC-MS method. J Labelled Comp Radiopharm 2014;57:606–10.
24. Itoh K, Chiba T, Takahashi S, Ishii T, Igarashi K, Katoh Y, et al. An Nrf2/small Maf heterodimer mediates the induction of phase II detoxifying enzyme genes through antioxidant response elements. Biochem Biophys Res Commun 1997;236:313–22.
25. Taguchi K, Maher JM, Suzuki T, Kawatani Y, Motohashi H, Yamamoto M. Genetic analysis of cytoprotective functions supported by graded expression of Keap1. Mol Cell Biol 2010;30:3016–26.
26. Prochaska HJ, Santamaria AB. Direct measurement of NAD(P)H:quinone reductase from cells cultured in microtiter wells: a screening assay for anticarcinogenic enzyme inducers. Anal Biochem 1988;169:328–36.
27. Habig WH, Jakoby WB. Glutathione S-transferases (rat and human). Methods Enzymol 1981;77:218–31.
28. McMahon M, Itoh K, Yamamoto M, Hayes JD. Keap1-dependent proteasomal degradation of transcription factor Nrf2 contributes to the negative regulation of antioxidant response element-driven gene expression. J Biol Chem 2003;278:21592–600.
29. Wade KL, Garrard IJ, Fahey JW. Improved hydrophilic interaction chromatography method for the identification and quantification of glucosinolates. J Chromatogr A 2007;1154:469–72.
30. Braun S, Hanselmann C, Gassmann MG, auf dem Keller U, Born-Berclaz C, Chan K, et al. Nrf2 transcription factor, a novel target of keratinocyte growth factor action which regulates gene expression and inflammation in the healing skin wound. Mol Cell Biol 2002;22:5492–505.
31. Dinkova-Kostova AT, Talalay P, Sharkey J, Zhang Y, Holtzclaw WD, Wang XJ, et al. An exceptionally potent inducer of cytoprotective enzymes: elucidation of the structural features that determine inducer potency and reactivity with Keap1. J Biol Chem 2010;285:33747–55.

Published OnlineFirst March 24, 2015; DOI: 10.1158/1940-6207.CAPR-14-0362

32. Grivennikov SI, Greten FR, Karin M. Immunity, inflammation, and cancer. Cell 2010;140:883–99.
33. Taniguchi K, Karin M. IL-6 and related cytokines as the critical lynchpins between inflammation and cancer. Semin Immunol 2014;26:54–74.
34. Liby K, Yore MM, Roebuck BD, Baumgartner KJ, Honda T, Sundararajan C, et al. A novel acetylenic tricyclic bis-(cyano enone) potently induces phase 2 cytoprotective pathways and blocks liver carcinogenesis induced by aflatoxin. Cancer Res 2008;68:6727–33.
35. Liu H, Dinkova-Kostova AT, Talalay P. Coordinate regulation of enzyme markers for inflammation and for protection against oxidants and electrophiles. Proc Natl Acad Sci U S A 2008;105:15926–31.
36. O'Donovan P, Perrett CM, Zhang X, Montaner B, Xu YZ, Harwood CA, et al. Azathioprine and UVA light generate mutagenic oxidative DNA damage. Science 2005;309:1871–4.
37. Gueranger Q, Li F, Peacock M, Larnicol-Fery A, Brem R, Macpherson P, et al. Protein Oxidation and DNA Repair Inhibition by 6-Thioguanine and UVA Radiation. J Invest Dermatol 2014;134:1408–17.
38. Kalra S, Knatko EV, Zhang Y, Honda T, Yamamoto M, Dinkova-Kostova AT. Highly potent activation of Nrf2 by topical tricyclic bis(cyano enone): implications for protection against UV radiation during thiopurine therapy. Cancer Prev Res 2012;5:973–81.
39. Karran P, Attard N. Thiopurines in current medical practice: molecular mechanisms and contributions to therapy-related cancer. Nat Rev Cancer 2008;8:24–36.
40. de Gruijl FR, Van der Leun JC. Estimate of the wavelength dependency of ultraviolet carcinogenesis in humans and its relevance to the risk assessment of a stratospheric ozone depletion. Health Phys 1994;67:319–25.
41. Dinkova-Kostova AT, Fahey JW, Wade KL, Jenkins SN, Shapiro TA, Fuchs EJ, et al. Induction of the phase 2 response in mouse and human skin by sulforaphane-containing broccoli sprout extracts. Cancer Epidemiol Biomarkers Prev 2007;16:847–51.
42. Dawe RS, Ibbotson SH, Sanderson JB, Thomson EM, Ferguson J. A randomized controlled trial (volunteer study) of sitafloxacin, enoxacin, levofloxacin and sparfloxacin phototoxicity. The British J dermatology 2003; 149:1232–41.
43. Crunkhorn S. Deal watch: Abbott boosts investment in NRF2 activators for reducing oxidative stress. Nat Rev Drug Discov 2012;11:96.
44. auf dem Keller U, Huber M, Beyer TA, Kumin A, Siemes C, Braun S, et al. Nrf transcription factors in keratinocytes are essential for skin tumor prevention but not for wound healing. Mol Cell Biol 2006;26:3773–84.
45. South AP, Purdie KJ, Watt SA, Haldenby S, den Breems NY, Dimon M, Arron ST, et al. NOTCH1 mutations occur early during cutaneous squamous cell carcinogenesis. J Invest Dermatol 2014;134:2630–8.
46. Schafer M, Willrodt AH, Kurinna S, Link AS, Farwanah H, Geusau A, et al. Activation of Nrf2 in keratinocytes causes chloracne (MADISH)-like skin disease in mice. EMBO Mol Med 2014;6:442–57.
47. Mitsuishi Y, Taguchi K, Kawatani Y, Shibata T, Nukiwa T, Aburatani H, et al. Nrf2 redirects glucose and glutamine into anabolic pathways in metabolic reprogramming. Cancer Cell 2012;22:66–79.
48. Singh A, Happel C, Manna SK, Acquaah-Mensah G, Carrerero J, Kumar S, et al. Transcription factor NRF2 regulates miR-1 and miR-206 to drive tumorigenesis. J Clin Invest 2013;123:2921–34.
49. DeNicola GM, Karreth FA, Humpton TJ, Gopinathan A, Wei C, Frese K, et al. Oncogene-induced Nrf2 transcription promotes ROS detoxification and tumorigenesis. Nature 2011;475:106–9.
50. Sayin VI, Ibrahim MX, Larsson E, Nilsson JA, Lindahl P, Bergo MO. Antioxidants accelerate lung cancer progression in mice. Sci Transl Med 2014;6:221ra15.

Published OnlineFirst March 24, 2015; DOI: 10.1158/1940-6207.CAPR-14-0362

AACR American Association for Cancer Research

Cancer Prevention Research

Nrf2 Activation Protects against Solar-Simulated Ultraviolet Radiation in Mice and Humans

Elena V. Knatko, Sally H. Ibbotson, Ying Zhang, et al.

Cancer Prev Res 2015;8:475-486. Published OnlineFirst March 24, 2015.